Intricacies of alpha-synuclein aggregation

Mucibabic, M.

Chapter 4

Influence of solution conditions on α-synuclein aggregation kinetics

Abstract

Parkinson's disease (PD) is a neurodegenerative disorder characterized by the presence of abnormal deposits of aggregated proteins known as Lewy bodies in brain tissue. The major components of Lewy bodies are aggregates of a small presynaptic protein known as α-synuclein (α-syn). Despite a significant research effort the mechanism of oligomer and fibril formation and the conditions which trigger the aggregation process are not well understood. The aim of this study was to determine the effect of solution conditions on seeded α-syn aggregation and fibril growth by the use of a Thioflavin T fluorescence assay. The relationship between α-syn elongation kinetics of ionic strength and pH was measured, and a detailed analysis is presented in terms of a kinetic model. The effect of pH and of salt concentration on elongation kinetics of preformed α-syn fibrils deviates significantly from their effect on the lag phase, suggesting that the mechanism for α-syn nucleation and fibril elongation are different.

4.1. Introduction

Amyloid fibrils are in the spotlight of the scientific community not only for their relevance in diseases such as Parkinson's and Alzheimer's disease [1], but also for their application in nanotechnology and biotechnology [2]. Discovering the steps in the conversion of functional proteins into amyloid fibrils [3] is crucial for understanding their origin and proliferation and for understanding how amyloid fibrils are associated with a range of health disorders [4]. The past decade has seen numerous theoretical and experimental studies attempting to determine and characterize the kinetic process involved in the self-assembly of amyloid proteins into fibrils [5–7]. However, the outcomes of the experiments often differ [8], which is usually connected to the heterogeneity in the early events of the fibrillization process. Interestingly, despite their very different primary peptide sequences, amyloid fibrils share common structural features, such as their micrometer length, twisted appearance [9,10] and rich β-sheet structure [11]. It has been reported that many amyloid fibrils, including α-syn, elongate by binding of monomers to fibril ends [12,13]. Mechanisms of the *de novo* fibril formation include oligomerization [14], fibril breaking [15–17] and fibril–catalyzed secondary nucleation [18].

Protein aggregation is often monitored using an assay based on the fluorescence enhancement of Thioflavin T (ThT) dye, which specifically binds to β-sheets structures [19]. It has been previously reported that a typical aggregation curve, as followed by ThT fluorescence, has a sigmoidal shape and is described by first order kinetics [20] (see Chapter 1, Figure 1.3). The aggregation curve is determined by nucleation (lag phase), growth (exponential phase) and saturation (plateau phase). During the lag phase initiation of aggregation occurs by forming the nuclei for the start of the reaction, described in the literature as primary nucleation [21]. At this stage there is no ThT fluorescence increase. The growth phase is characterized by exponential growth of the ThT fluorescence. Several processes are underlying it, such as elongation of existing aggregates by monomer addition to fibril end(s) [22] and formation of new growing centers by breaking of existing fibrils [15] – so called secondary nucleation. In the saturation phase ThT fluorescence reaches a plateau, where most of the monomer pool has been depleted by incorporation into aggregates [3] and the rate of the monomer addition to the fibril ends is equal to the dissociation rate. The time scale for primary nucleation of α-syn aggregation is highly variable, and though the nucleation phase is most important in the aggregation process it is still not very well understood. Concerning the overall mechanism of

α-syn aggregation, the rate-limiting steps, the role and nature of intermediates still remain not well elucidated [5,6,8]. The lag phase that represents the primary nucleation [6] can be largely eliminated by using preformed fibrils (seeds) and, provides a convenient way to focus especially on the elongation reaction of α-syn fibrils.

Effects of solution conditions on α-syn aggregation were studied by bulk experiments [23,24] and atomic force microscopy [25]. In the study by Hoyer and coworkers [23] the effect of solution conditions on the overall rate of α-syn aggregation was reported, together with the change in aggregate morphology, especially at low pH. Their finding indicates that adding 200 mM NaCl can accelerate the formation of aggregation nuclei [21]. Buell et al. [13] showed that primary and secondary nucleation govern the proliferation of aggregates at pH 7, with secondary nucleation being particularly prominent at pH below 6. They also reported that the fibril elongation rate is strongly influenced by the salt concentration. As α-syn aggregation kinetics and morphology depend significantly on pH, ionic strength, temperature etc., it is important to determine which phase of the process is affected the most and to gain new information about it.

Here we report to what extent the fibrillar growth phase of α-syn aggregation is affected by solution conditions, in particular ionic strength and pH, based on a recording of the α-syn fibril elongation kinetics in bulk. The bulk fibrillar growth was monitored by the ThT assay, and the average initial elongation rate of the fibrils was measured. To skip largely the nucleation phase and focus on fibril elongation only, we monitored WT α-syn in the presence of preformed fibrils (seeds). Under those conditions the lag phase is effectively suppressed in the growth kinetics. The present study resulted in direct experimental evidence that the initial elongation rate of the α-syn fibrils increases at relatively low concentrations of sodium chloride (up to 30 mM NaCl) and decreases at higher NaCl concentrations. No particular trend is observed in the pH dependence of the initial growth rate, consistent with earlier reports [13].

4.2. Materials and Methods

4.2.1. Expression and purification of α-syn

Preparation and purification of α-syn was performed as described elsewhere [26]. WT α-syn was expressed in *E.coli* BL21 (DE3) transformed with the pT7-7 plasmid carrying the α-syn gene. Culturing was done in lysogeny broth medium with 100 µg/ml ampicillin. After

induction by addition of isopropylthio-β-galactoside (1 mM, 4 h) bacterial cell pellets were harvested by centrifugation (6,000 × g, 10 min), resuspended in 10 mM Tris–HCl, pH 8.0, 1 mM ethylenediaminetetraacetic acid (EDTA) and 1mM phenylmethylsulfonyl fluoride (10% of the culture volume) and stirred for 1 h at 4°C. Cells were lysed by sonication for 2 min and centrifuged (10,000 × g, 20 min, 4°C).

By adding streptomycin sulfate (1%, 15 min, 4°C) DNA was precipitated and removed by centrifugation at 13,500 × g for 30 min. Next, α-syn was salted out from the solution by slowly adding ammonium sulfate up to a concentration of 0.295 g/ml and mild stirring (1 h, 4°C). Precipitated α-syn was collected by centrifugation (13,500 × g, 30 min, 4°C). The pellet was gently resuspended in 10 mM Tris–HCl, pH 7.4 and the solution was eluted over a 6 ml ResourceQ anion exchange column (GE Healthcare) using the Äkta Purifier system (GE Healthcare) and a linear gradient of NaCl (0–500 mM) in 10 mM Tris–HCl, pH 7.4 at a flowrate of 3 ml/min. Fractions containing α-syn (eluted at ~300 mM NaCl) were pooled, concentrated (Vivaspin-20, 10 kDa; GE Healthcare) and desalted using a PD-10 column (GE Healthcare) in 10 mM Tris–HCl pH 7.4 (containing 1 mM DTT in the case of cysteine mutant). Protein concentration was determined on the basis of the tyrosine absorption at 275 nm by using 5600 M^{-1} cm^{-1} for the extinction coefficient of WT [24].

4.2.2. Kinetic model of aggregation

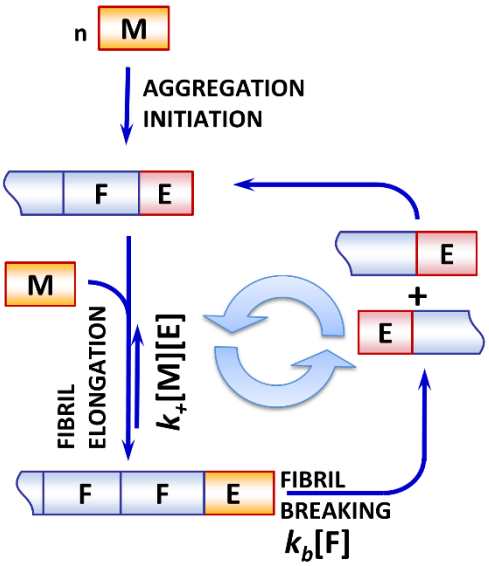

Figure 4.1: Kinetic model of α-syn aggregation, which includes three steps: initiation, growth and formation of new fibril ends, where [M] is the monomer concentration, [E] the concentration of active growing ends, [F] the amount of fibrillar α-syn, k_+ the elongation rate and k_b the breaking rate (Figure reprinted with permission from 15 given by ACS Publications).

The data were analyzed with a kinetic model which is described in detail elsewhere [15]. In this proposed model [15] α-syn aggregation includes three steps (see Figure 4.1). It starts with an initial phase, where new aggregates are formed spontaneously and it continues with a growth phase, where mostly monomers bind to existing fibril ends and fibrils get elongated. The fluorescence intensity growth is nonlinear, and upon monomer depletion slows down. During the aggregation process, especially under agitation, fibrils can break which produces new fibril ends. In the presence of seeds and at the time scale of the experiments reported here, the initial increase in ThT fluorescence is governed by seed elongation. Ignoring the primary nucleation, seed elongation can be described by following equation:

$$\frac{\Delta F(t)}{\Delta t} = \frac{F_t - F_0}{(t - t_0)} = k_+[M][E]$$

Here $\Delta F(t)$ is the change in concentration of fibrillized protein during the time interval of Δt, F_0 is the concentration of the fibrillized protein at t_0 while F_t is the concentration of the fibrillized protein at a later time t. The change in fluorescence intensity is converted to equivalent monomer concentration by scaling to the intensity in the plateau phase where we assume that all α-syn is in aggregated form. [M] is the monomer concentration, [E] the seed concentration and k_+ the fibril elongation rate. The initial elongation rate was measured by following the increase of the ThT signal during the first 30000 s of the measurement, where the increase in the ThT fluorescence was linear in time. It was assumed that during the first 30000 s fibril breaking did not occur which means that [E] is essentially constant. Longer fibrils are more prone to breaking, but during the first 30000 s of seed elongation long fibrils are not common. Control experiments under identical conditions, but in the absence of seeds, showed that at this time scale primary nucleation did not make a significant contribution to the ThT signal. Thus we have for k_+:

$$k_+ = \frac{F_t - F_0}{(t - t_0)\,[M][E]}$$

The units of k_+ are $mM^{-1}\,s^{-1}$.

4.2.3. Kinetic measurements and the aggregation model

The aggregation experiments were performed in a Tecan Infinite M200pro plate reader and seed elongation was monitored by recording the ThT fluorescence. All experiments were performed at 37°C, under shaking conditions (300 s of linear shaking with 6 mm amplitude)

in 384 well plates (Nunc, Thermo Fisher Scientific) sealed with a transparent, polyolefin film (Viewseal, Greiner Bio One) to avoid evaporation, using a volume of 50 µL per well. The final solution used for aggregation contained 6 mM sodium phosphate buffer at pH 4-10, 0-200 mM NaCl, 9 mM NaN_3, 0.1 mM EDTA (to remove divalent ions), and 5 µM ThT (≥ 5% of α-syn concentration). The α-syn monomer concentration was 100 µM unless otherwise indicated. Samples were measured in at least 8 replicates. Fluorescence of ThT was always recorded from the bottom of the plate. Excitation was at 446 nm, emission at 485 nm, excitation and emission spectral bandwidths were set at 9 and 20 nm, respectively.

A solution of mature α-syn fibrils was obtained by combining four separately aggregated 100 µM α-syn samples that had reached the plateau phase of ThT fluorescence, all grown under the same experimental conditions, in 6 mM phosphate buffer pH 7.2 with 150 mM NaCl, at 37°C, using constant agitation.. A stock solution of seeds was obtained by sonicating approximately 200 µl of this solution of mature fibrils for 300 s in a water bath sonicator (VWR 75D ultrasonic cleaner, power 90 W, bath volume 2.5 L). All experiments were performed with the same stock solution of seeds.

4.3. Results

4.3.1. Initial aggregation rate at different salt concentrations

To determine to what extent the ionic strength of the solution has an influence on α-syn elongation the NaCl concentration was varied in the range of 0 to 200 mM. For this purpose WT α-syn seeds were added to a solution of 100 µM WT α-syn monomers, with a final concentration of 0.16 nM. The initial elongation rate was determined based on the increase of the ThT fluorescence signal in time during the first 30000 s as described in Materials and Methods, applying the kinetic model established by Shvadchak and coworkers [15].

shows the dependence of the average initial elongation rate on NaCl concentration. The error bars denote standard deviations of the initial elongation rate. The data show that the average initial elongation rate increases with increasing NaCl concentrations up to 30 mM NaCl and decreases after that.

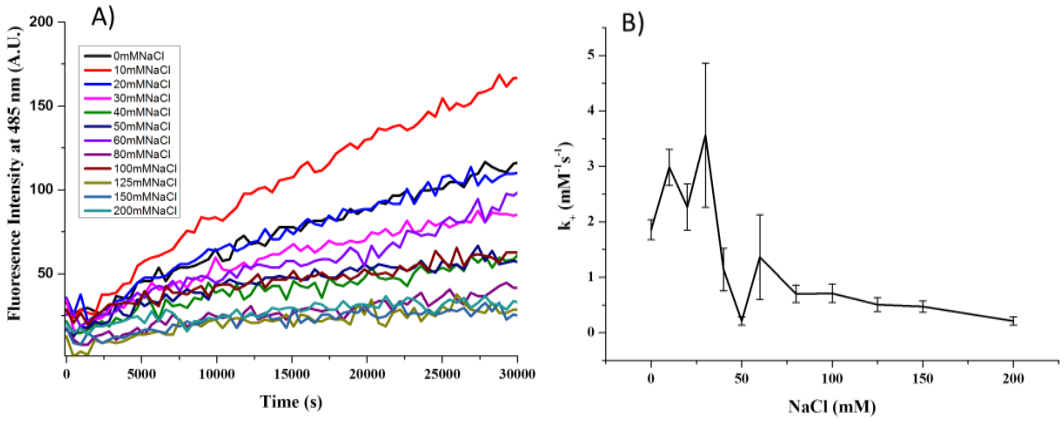

Figure 4.2: (A) Initial elongation kinetics of WT α-syn seeds before secondary nucleation sets in, measured by ThT fluorescence. Each curve is an average of 8 samples. (B) The initial elongation rate as a function of NaCl concentration. The initial elongation rate decreased with NaCl concentrations above 30 mM. All measurements were performed under the same conditions: samples contained 0.16 nM α-syn preformed seeds in the presence of 100 µM α-syn, 6 mM sodium phosphate buffer at pH 7.2, 0-200 mM NaCl, and 0.1 mM EDTA, at 37°C, under shaking. The error bars represent the standard deviation.

4.3.2. Initial aggregation rate as a function of pH

Previous studies reported structural changes of α-syn when the pH was varied [27], differences in aggregate morphology between pH 4 and 7 [21] and variation of fibril growth kinetics in going from neutral to lower pH [13]. However, detailed information about the kinetics of fibrillar growth from seeds as a function of pH is still incomplete and we aimed to test the effect of a wider range of pH values on α-syn elongation. Our experiments were performed in 6 mM sodium phosphate buffer from pH 4 to 10 in the presence of 0 and of 150 mM NaCl, respectively, while keeping constant the other experimental conditions such as protein and seeds concentration, temperature and shaking.

Figure 4.3 shows the initial elongation rates of α-syn seeds as a function of pH, where the red and black symbols apply to 0 and 150 mM NaCl respectively. In general, the average initial elongation rates are higher in case of the former.

4.4. Discussion

Using the ThT aggregation assay in the presence of preformed fibrils (seeds) we observed that the average initial elongation rate of α-syn showed a pronounced dependence on salt concentration. The highest average initial elongation rate was measured at 30 mM NaCl. It is concluded that electrostatic interactions play an important role during the elongation process. In general, proteins can be stabilized or destabilized by the presence of salts in solution. This

may also apply to the range of conformational structures that α-syn can adopt. The high negative charge of the C-terminal domain will be effectively screened at high salt concentrations which will affect Coulombic intra- and intermolecular interactions.

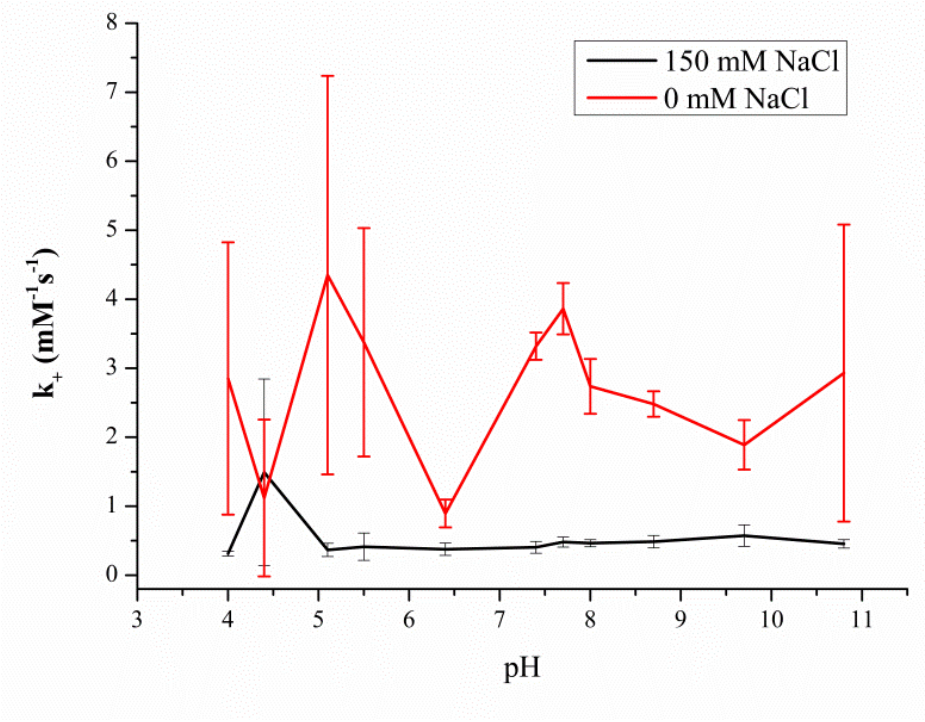

Figure 4.3: Dependence of the initial elongation rate on pH of 0.16 nM WT α-syn seeds in the presence of 100 µM WT α-syn monomers at two different NaCl concentrations, obtained from plate reader measurements. Black: 150 mM NaCl, red: 0 mM NaCl. The error bars show the standard deviation of the initial elongation rate of 8 replicates.

This point has been used to explain the effect of salt on the aggregation rate of (monomeric) α-syn [28] and to account for the different conformations reported for α-syn at 0 and 150 mM, respectively [29]. At high salt concentrations α-syn aggregates assemble within hours, whereas the lag phase extends to several days under low-salt conditions [25,29]. Moreover, these two salt conditions result in different fibril morphologies. In a recent study employing 19F-NMR Bai et al. [28] showed that α-syn adopts a more compact structure in the absence of NaCl, consistent with a reduced hydrodynamic radius [29]. Long-range interaction of the C-terminal with the N-terminal domain appears to play a key role.

The data on the pH dependence of the initial elongation rate of α-syn seeds (Figure 4.3) do not show a clear trend in the data other than that the measured rates are higher in the case of 0 mM NaCl. In the mild acidic range we observe a relatively large standard deviation in the results from 8 replicate measurements. We attribute this spread in the rates to the fact that secondary nucleation can probably not be neglected under the shaking conditions in the present experiments. Buell et al. [13], for example, have shown that the rate of secondary

nucleation increases dramatically in going from neutral to pH 5.2. In line with their results we conclude that the initial elongation rate of α-syn seeds does not show a strong variation in the range of pH 4 to 8 at 150 mM NaCl, although at 0 mM NaCl the initial elongation rates do vary somewhat with pH.

This is in contrast to an earlier report by Uversky et al. [30], where it was shown that the rate of fibrillization of α-syn was strongly pH dependent. In their case, however, the experiment involved the aggregation kinetics of monomers in solution and the data show that the pH dependence is dominated by the variation in lag time. They concluded that a decrease in pH leads to the formation of a precursor, possibly a partially folded intermediate, with a strongly enhanced propensity for the formation of α-syn fibrils [30]. Indeed, it is generally assumed that conformational intermediates play a key role in the nucleation dependent pathway of α-syn aggregation. The large change in net charge of α-syn and in its internal charge distribution as a function of pH is believed to be involved in concomitant changes of the molecular conformation associated a collapse of the normally highly acidic and extended C-terminal tail at low pH [27]. Most likely as a result of long-range interactions α-syn at low pH appears to adopt a more compact conformation, which presumably exhibits a larger rate of aggregation [30].

However, this precursor or intermediate does not lead to enhancement of the elongation rate of existing fibrils according to our conclusion above. Thus, we surmise that the affinity of this intermediate to bind to the fibril end is not significantly affected by the pH. This suggests that the mechanism of nucleation is possibly different from that of fibril elongation. An explanation may be that the α-syn fibrils are stabilized by a change of conformation of the constituent initial aggregate, i.e., the fibrillar template is formed in a secondary step after nucleation. Such a conformational change may lead to a different reactivity for binding of α-syn monomers to the fibril end compared to primary nucleation.

These previous reports [25,29,30] build a strong case for the effect of solution conditions on the α-syn monomeric structure. Thus, solution conditions may affect the kinetics of fibril formation and fibril morphology. We note, however, that they specifically apply to measurements of aggregation in monomeric α-syn solutions and that they show that in particular the duration of the lag phase is affected by the presence of salt [6,25,29].

The results in Figure 4.2 apply to seeded aggregation where the lag phase is largely absent, and where the initial rate is dominated by fibril elongation. Here the difference in rates is significant between low salt (0 mM NaCl) and high salt (~150 mM NaCl) conditions, but the highest at 30 mM NaCl. Presumably the α-syn monomer addition to the fibril end involves a different molecular conformation than the one which promotes nucleation, being stabilized at the lower salt concentration of around 30 mM and that might point to the different nucleation and elongation mechanism.

4.5. Conclusion

Our results address the effect of solution conditions on the seeded aggregation of α-syn by using the ThT fluorescence assay. The effect of pH on the initial elongation rate is not significant, in contrast to its effect on the lag phase. Also the influence of salt on the elongation rate deviates from that on the lag phase. Both observations suggest that the nucleation and elongation proceed by different mechanisms.

Acknowledgements

We thank Ms. N. Schilderink from University of Twente for α-synuclein expression and purification and Dr. Volodymyr Shvadchak for his help with data analysis. This work was performed in the research program entitled ‘‘A Single Molecule View on Protein Aggregation’’, supported by the Foundation for Fundamental Research on Matter (FOM), which is part of the Netherlands Organization for Scientific Research (NWO).

4.6. References

[1] C.M. Dobson, Alzheimer's disease: addressing a twenty-first century plague, Rend. Lincei. 26 (2015) 251–262. doi:10.1007/s12210-015-0453-y.

[2] S. Mankar, A. Anoop, S. Sen, S.K. Maji, Nanomaterials: amyloids reflect their brighter side, Nano Rev. 2 (2011) 1–12. doi:10.3402/nano.v2i0.6032.

[3] S.I.A. Cohen, M. Vendruscolo, C.M. Dobson, T.P.J. Knowles, From macroscopic measurements to microscopic mechanisms of protein aggregation, J. Mol. Biol. 421 (2012) 160–171. doi:10.1016/j.jmb.2012.02.031.

[4] F. Chiti, C.M. Dobson, Protein misfolding, functional amyloid, and human disease., Annu. Rev. Biochem. 75 (2006) 333–366. doi:10.1146/annurev.biochem.75.101304.123901.

[5] T.P.J. Knowles, C.A. Waudby, G.L. Devlin, S.I.A. Cohen, A. Aguzzi, M. Vendruscolo, et al., An analytical solution to the kinetics of breakable filament assembly., Science. 326 (2009) 1533–1537. doi:10.1126/science.1178250.

[6] P. Arosio, T.P.J. Knowles, S. Linse, On the lag phase in amyloid fibril formation, Phys. Chem. Chem. Phys. 17 (2015) 7606–7618. doi:10.1039/C4CP05563B.

[7] S. Prigent, A. Ballesta, F. Charles, N. Lenuzza, P. Gabriel, L.M. Tine, et al., An Efficient Kinetic Model for Assemblies of Amyloid Fibrils and Its Application to Polyglutamine Aggregation, PLoS One. 7 (2012) 1–9. doi:10.1371/journal.pone.0043273.

[8] L. Giehm, D.E. Otzen, Strategies to increase the reproducibility of protein fibrillization in plate reader assays, Anal. Biochem. 400 (2010) 270–281. doi:10.1016/j.ab.2010.02.001.

[9] M.E. van Raaij, J. van Gestel, I.M.J. Segers-Nolten, S.W. de Leeuw, V. Subramaniam, Concentration dependence of alpha-synuclein fibril length assessed by quantitative atomic force microscopy and statistical-mechanical theory., Biophys. J. 95 (2008) 4871–4878. doi:10.1529/biophysj.107.127464.

[10] A. Sidhu, I. Segers-Nolten, V. Subramaniam, Solution conditions define morphological homogeneity of α-synuclein fibrils., Biochim. Biophys. Acta. 1844 (2014) 2127–2134. doi:10.1016/j.bbapap.2014.09.007.

[11] D. Eisenberg, M. Jucker, The Amyloid State of Proteins in Human Diseases, Cell. 148 (2012) 1188–1203. doi:10.1016/j.cell.2012.02.022.

[12] D. Pinotsi, A.K. Buell, C. Galvagnion, C.M. Dobson, G.S. Kaminski Schierle, C.F. Kaminski, Direct observation of heterogeneous amyloid fibril growth kinetics via two-color super-resolution microscopy, Nano Lett. 14 (2014) 339–345. doi:10.1021/nl4041093.

[13] A.K. Buell, C. Galvagnion, R. Gaspar, E. Sparr, M. Vendruscolo, T.P.J. Knowles, et al., Solution conditions determine the relative importance of nucleation and growth processes in α-synuclein aggregation., Proc. Natl. Acad. Sci. U. S. A. 111 (2014) 7671–7676. doi:10.1073/pnas.1315346111.

[14] A.T. Sabareesan, J.B. Udgaonkar, Amyloid fibril formation by the chain B subunit of monellin occurs by a nucleation-dependent polymerization mechanism., Biochemistry.

53 (2014) 1206–17. doi:10.1021/bi401467p.

[15] V.V. Shvadchak, M.M.A.E. Claessens, V. Subramaniam, Fibril Breaking Accelerates α-Synuclein Fibrillization, J. Phys. Chem. B. 119 (2015) 1912–1918. doi:10.1021/jp5111604.

[16] S.R. Collins, A. Douglass, R.D. Vale, J.S. Weissman, Mechanism of prion propagation: Amyloid growth occurs by monomer addition, PLoS Biol. 2 (2004). doi:10.1371/journal.pbio.0020321.

[17] V. Meyer, P.D. Dinkel, E. Rickman Hager, M. Margittai, Amplification of Tau fibrils from minute quantities of seeds., Biochemistry. 53 (2014) 5804–9. doi:10.1021/bi501050g.

[18] S.I.A. Cohen, S. Linse, L.M. Luheshi, E. Hellstrand, D. A. White, L. Rajah, et al., Proliferation of amyloid- 42 aggregates occurs through a secondary nucleation mechanism, Proc. Natl. Acad. Sci. 110 (2013) 9758–9763. doi:10.1073/pnas.1218402110.

[19] H. LeVine, Thioflavine T interaction with synthetic Alzheimer's disease beta-amyloid peptides: detection of amyloid aggregation in solution., Protein Sci. 2 (1993) 404–410. doi:10.1002/pro.5560020312.

[20] S.J. Wood, J. Wypych, S. Steavenson, J. Louis, M. Citron, A.L. Biere, a-Synuclein Fibrillogenesis is Nucleation-dependent, Biochemistry. (1999) 19509–19512.

[21] C. Galvagnion, A.K. Buell, G. Meisl, T.C.T. Michaels, M. Vendruscolo, T.P.J. Knowles, et al., Lipid vesicles trigger α-synuclein aggregation by stimulating primary nucleation, Nat. Chem. Biol. 11 (2015) 229–234. doi:10.1038/nchembio.1750.

[22] R. Khurana, C. Ionescu-Zanetti, M. Pope, et al., A general model for amyloid fibril assembly based on morphological studies using atomic force microscopy., Biophys. J. 85 (2003) 1135–44. doi:10.1016/S0006-3495(03)74550-0.

[23] L.A. Munishkina, J. Henriques, V.N. Uversky, A.L. Fink, Role of Protein - Water Interactions and Electrostatics in α-Synuclein Fibril, (2004) 3289–3300.

[24] V.N. Uversky, J. Li, A.L. Fink, Metal-triggered structural transformations, aggregation, and fibrillation of human α-synuclein: A possible molecular link between parkinson's disease and heavy metal exposure, J. Biol. Chem. 276 (2001) 44284–44296. doi:10.1074/jbc.M105343200.

[25] W. Hoyer, T. Antony, D. Cherny, G. Heim, T.M. Jovin, V. Subramaniam, Dependence of α-synuclein aggregate morphology on solution conditions, J. Mol. Biol. 322 (2002) 383–393. doi:10.1016/S0022-2836(02)00775-1.

[26] M. Mučibabić, M.M. Apetri, G.W. Canters, T.J. Aartsma, The effect of fluorescent labeling on α-synuclein fibril morphology, Biochim. Biophys. Acta - Proteins Proteomics. (2016). doi:10.1016/j.bbapap.2016.07.007.

[27] S. McClendon, C.C. Rospigliosi, D. Eliezer, Charge neutralization and collapse of the C-terminal tail of alpha-synuclein at low pH, Protein Sci. 18 (2009) 1531–1540. doi:10.1002/pro.149.

[28] J. Bai, K. Cheng, M. Liu, C. Li, Impact of the α-Synuclein Initial Ensemble Structure on Fibrillation Pathways and Kinetics, J. Phys. Chem. B. 120 (2016) 3140–3147. doi:10.1021/acs.jpcb.6b01225.

[29] L. Bousset, L. Pieri, G. Ruiz-Arlandis, J. Gath, P.H. Jensen, B. Habenstein, et al., Structural and functional characterization of two alpha-synuclein strains., Nat. Commun. 4 (2013) 2575. doi:10.1038/ncomms3575.

[30] V.N. Uversky, Evidence for a Partially Folded Intermediate in alpha-Synuclein Fibril Formation, J. Biol. Chem. 276 (2001) 10737–10744. doi:10.1074/jbc.M010907200.